Published in final edited form as:
IEEE Trans Biomed Eng. 2008 March ; 55(3): 996–1003. doi:10.1109/TBME.2007.906489.

A Novel Angiographic Methodology for the Quantification of Angiogenesis

Matthew J. Gounis,
Department of Radiology, University of Massachusetts, 55 Lake Avenue N, SA-170R, Worcester, MA 01655 USA (Matt.Gounis@umassmed.edu).

Baruch B. Lieber,
Vascular Biology Institute, University of Miami, Miami, FL 33136 USA and also with the Department of Biomedical Engineering and the Department of Radiology, University of Miami, Coral Gables, FL 33146 USA (blieber@miami.edu).

Keith A. Webster, and
Vascular Biology Institute and the Department of Molecular Pharmacology, University of Miami, Miami, FL 33136 USA (kwebster@med.miami.edu).

Ajay K. Wakhloo
Department of Radiology, University of Massachusetts, Worcester, MA 01655 USA (WakhlooA@ummhc.org).

Abstract

The objective is to develop a method to quantify the dynamic information of contrast transport using angiography for investigating angiogenic treatments. In the rabbit hindlimb ischemia model, contrast media transport was examined for both arteries and the microvasculature. Time histories of image intensity were constructed and modeled. The differences in contrast transport quantified by the parameters of the mathematical model were statistically compared between animals treated with an adenoviral vector that expressed vascular endothelial growth factor and untreated animals. The data reveal that after one week of ischemia, treated animals have a statistical increase in the number of large vessels that convect blood more efficiently. This analysis further shows a statistically significant increase in the angiographic blush in the treated animals. A methodology is described that offers the capability of examining the number and geometry of large arteries, the dynamics of contrast transport, and the amount of angiographic blush that is related to microvascular density. In therapeutic angiogenesis, numerous techniques are used to measure variables such as the angiographic score, capillary density, and regional blood flow. The analysis presented herein can offer information of these variables, and is transferable from the laboratory to the clinical arena.

Index Terms

Angiogenesis; angiography; gene therapy; ischemia; mathematical modeling

Correspondence to: Matthew J. Gounis.

I. Introduction

Peripheral arterial disease (PAD) threatens the survival of extremities and often causes lifelong disablement (reviewed in [1] and [2]). The incidence of PAD in the U.S. is estimated at over 300 000 new patients per year, and the prognosis for many of these patients is poor. The clinical consequences include claudication, pain at rest and loss of tissue integrity in the distal limbs that might lead to amputation. Intermittent claudication affects more than 5% of people over 50 years of age and has a variable outcome with symptoms progressing rapidly in 25% of patients and almost 10% requiring amputations within five years. Progressive deterioration to rest pain or gangrene occurs in about 20% of all patients with intermittent claudication. The life expectancy of amputees is less than five years.

Evidence from both animal and patient studies indicate that risk factors for PAD, in particular age, diabetes, and hyperlipidemia are associated with depressed levels of angiogenic growth factors including vascular endothelial growth factor [3]. Growth factor deficiency and depressed angiogenic potential may therefore contribute to the establishment and progression of arterial disease. Therapeutic angiogenesis involves the introduction of exogenous growth factor proteins, genes, or stem cells directly into the diseased tissues to augment endogenous factors and promote new vessel growth (reviewed in [4]–[7]). Therapeutic angiogenesis is currently being tested as a treatment for PAD and coronary artery disease. Results from studies in animal models initiated in the early 1990s were encouraging and have provided support for multiple clinical trials testing vascular endothelial growth factor (VEGF) and fibroblast growth factor (FGF) proteins and genes [8]–[11].

Angiographic assessment of angiogenesis is the standard method for evaluating the vasculature and production of collateral vessels in response to therapeutic angiogenesis, but the technique is limited to the analysis of singular angiographic images. The most common imaging technique used to quantify outcomes of proangiogenic therapy is the calculation of an angiographic score. A novel approach has been developed and is described herein, to quantify the level of angiogenesis by modeling the temporal variation of contrast intensity throughout an angiographic sequence. The dynamic information extracted from the images of angiographic sequences may then be mathematically modeled, and the model parameters provide information about the transport of contrast through the specified region of interest (ROI). The hypothesis is that these model parameters serve as quantifiable indices of the efficacy of therapeutic angiogenesis.

II. Materials and Methods

A. Animal Model

All *in vivo* procedures described herein were performed with rabbits under general anesthesia. All *in vivo* procedures were conducted in accordance with the guidelines of the Animal Care and Use Committee at the University of Miami. A total of 12 rabbits are included in this study, six each in the control and treated groups.

The rabbit hindlimb ischemia model is commonly employed to study proangiogenic treatment. The left external iliac artery was ligated approximately 2 cm distal to the internal/external iliac bifurcation at the level of the inguinal ligament. After isolation of the site of iliac ligation, a 2-cm segment of the left femoral artery distal to the lateral femoral circumflex artery and proximal from the descending genicular artery was resected. Fig. 1 depicts the arterial vasculature of the rabbit before and after the induction of ischemia.

The treated group received total intramuscular injection of 600 μL of a suspension of 1×10^{10} pfu of an adenoviral vector encoded to express $VEGF_{165}$ at ten randomly selected sites throughout the medial aspect of the thigh muscles. The recombinant AV vector was manufactured from a replication deficient type-5 AV lacking the E1 and E3 loci [12]. The $VEGF_{165}$ cDNAs were inserted in place of the E1 region and expression was driven by the human cytomegalovirus promoter. The control group received like injections of sterile phosphate buffered saline (PBS).

B. Angiography

Prior to the induction of hindlimb ischemia, baseline angiographic runs of the normal hindlimb vasculature were obtained. The right common carotid artery (CCA) was exposed, and a 4-Fr hemostatic introducer sheath was then placed into the right CCA in a retrograde fashion. To prevent thromboembolic complications, anticoagulation therapy was administered with a bolus of 100 units/kg of heparin given intraarterially. Similar experiments to examine the *in vivo* angiogenic potential of VEGF explicitly do not employ heparin to avoid the suspected stimulatory effect of heparin on neovascularization [13]. However, it has been shown that heparin does not significantly alter the formation of collateral vessels in the rabbit hindlimb ischemia model [14]. A 4-Fr straight, infusion catheter with five side-holes (Tempo, Cordis Endovascular, Miami Lakes, FL) was navigated over a 0.035 inch Glidewire (Boston Scientific/MediTech, Natick MA) into the descending aorta. The final position of the catheter tip was at the level of the lumbar intervertebral disc between L5 and L6.

All angiographic studies were performed using a Siemens Angiostar Plus vascular imaging system (Siemens, Forchheim Germany). High-speed angiographic runs of the left lower limb were acquired at 30 frames per second and recorded as digital images with a resolution of 512 × 512 pixels. The acquired images had a depth of 8 bits. Injections of 5 cc of Visipaque-320 (GE Healthcare, Princeton, NJ) were performed at a rate of 3.0 cc/s by a computer-controlled microinjection system that has an accuracy of 0.25 μL. Pressure injection profiles were periodically recorded to ensure repeatability.

High-speed angiographic sequences were acquired before and after ischemia was induced surgically, and hitherto referred to as baseline and postsurgical (PS), respectively. After this initial procedure, the right CCA proximal to the arterial port was ligated and the neck and leg wounds were closed with continuous suture lines. At the follow-up angiography session, catheterization was performed precisely as described previously with access obtained in the left CCA. After the follow-up angiographic sequences were obtained, the animal was euthanized with an overdose of sodium pentobarbital (100 mg/kg, IV). The relevant muscles and randomly selected organs were resected postmortem for future immunohistochemical analysis.

C. Image Processing

The acquired images were imported into Matlab (The Mathworks Inc, Natick MA) for further image processing and analysis.

For repeatable analysis, the femur was isolated [Fig. 2(A)] from each sequence. The image containing only the femur was thresholded, converted to a binary image [Fig. 2(B)] and then skeletonized [Fig. 2(C)]. The resulting image of the skeletonized femur was used to create the initial mask. The magnitude of the major axis of the ellipse was 150% of the length of the cord connecting the endpoints of the skeletonized femur. The minor axis of the ellipse was 75% of the major axis. An example of the resulting ellipse is presented in Fig. 2(D). The ellipse then served as a polygonal region of interest, removing portions of the image

that extend beyond the boundaries of the ellipse. The image mask isolated an anatomical region of the rabbit hindlimb that allows for consistent comparisons to be made between different angiographic sequences.

Therapeutic proangiogenic therapy mediated by exogenous administration of VEGF or genes encoded to express VEGF induces the formation of neovasculature consisting of vessels in the range of 200–800 μm [8]. It has been reported that the majority of these new vessels have diameters closer to the lower limit of this range [8]. In these experiments, the smallest feature that may be resolved is approximately 250 μm. To ascertain the contribution of the larger vessels, having diameters greater than 250 μm, to the neovasculature, a large artery mask was created. The image representing the peak opacification of the large arteries was isolated and used to form the large artery mask. Five of the binary images preceding and following this peak opacified image were summed. Finally, the normalized, summed image was multiplied by the elliptical ROI mask, to create the large artery mask (LAM) [Fig. 3(A)]. To examine the smaller arteries which contribute to the angiographic blush, a blush mask [Fig. 3(B)] was created by inverting the pixel values of the previous LAM. Angiographic blush refers to a general darkening, or a decrease in image intensity, of the angiograms without clear delineation of vessels' boundaries. Using the blush mask, the subsequent analysis allowed for investigation of microvasculature changes in response to therapy Both the LAM and blush masks were applied to all acquired images and the temporal variations of image intensity were quantified for both regions.

D. Mathematical Modeling

After multiplying all images of a given angiographic sequence by its corresponding LAM, the average inverted intensity was calculated for each of the new grayscale images. The intensity values of the image ranged between 0 and 1. The mean grayscale intensity was determined for each image, subtracted from 1, and then normalized by the total image area divided by the number of pixels with a value of unity in the relevant LAM. Time intensity curves represented the time history of the average, inverted grayscale values (AIGV) throughout the observation period. To create the time intensity curves for the temporal variation of grayscale values within the microvessels, the exact same procedure was repeated using the blush mask.

For each rabbit, time intensity curves were calculated using both masks at three time points, namely before and after the surgical induction of ischemia and at the follow-up evaluation.

To quantify changes in the shape of the time intensity curves, the data were mathematically modeled, and the model fit was then optimized using an algorithm that minimizes the differences between the model and the data, in a least squares sense.

The particular model used in this study is based on that previously employed to examine the transport of contrast from intracranial aneurysms [15], [16]. The model has been adapted to more aptly describe the flow through a vascular bed, rather than within the specialized case of an aneurismal dilatation. The model combined two functions, namely a lagged normal density function and a modified error function

$$I(t)=\rho_1 \underbrace{\int_0^t \left[\frac{1}{\sigma\sqrt{2\pi}}\exp\left(\frac{-(\eta-\mu)^2}{2\sigma^2}\right)\frac{1}{\tau}\exp\left(\frac{-\eta}{\tau}\right)\right]d\eta}_{\text{Lagged Normal Probability Density Function}} + \rho_2 \underbrace{\int_0^t \frac{1}{\sigma\sqrt{2\pi}}\exp\left(\frac{-(\eta-\mu)^2}{2\sigma^2}\right)d\eta}_{\text{Modified Error Function}}.$$

Equation (1) represents the mathematical equation employed to mode the time intensity data aquired during the experiments. The lagged normal density function is the time convolution of a normal probability distribution function and an exponential decay. The normal component of the lagged normal density function modeled the temporal dispersion of contrast as a symmetric, random distribution about a mean (μ) with a standard deviation σ [17]. This component of the model was physically representative of the input, which is the injection of contrast. The second component of the lagged normal function is a monoexponential decay that is representative of contrast mixing with blood [17]. The lagged normal model adequately described the bulk fluid motion of contrast through the region of interest during the rise, early, and middle decay portions of the time intensity curves. However, this model dictated that the intensity values return to the background value within the observation period during the late decay phase. In this study, the observation period of less than 20 s was insufficient to allow the complete evacuation of contrast from the regions of interest. Thus, another mathematical function was superposed to account for the late decay phase of the time intensity curve.

The second term of the model, which is the integral of the normal probability density function, accounted for the contrast that remained during the late decay phase of the time intensity curves. This term, which is related by a constant to the error function, physically represented the multiple phenomena that lead to the departure of intensity from the background values at the end of the observation period. These phenomena included contrast stagnation, fluid entrainment of the contrast within the catheter and venous return.

The model parameters of (1) each had an understood contribution to the final shape of the model, which represented the transport of contrast. The amplification coefficients, ρ_1 and ρ_2, determined the relative contribution of each function to the amplitude of the inverted average grayscale value. These coefficients represented the total amount of contrast that was transported through the regions of interest. For consistent and repeatable injections of equal quantities of contrast material, the summed coefficients indicated the resistance of the vascular bed.

The standard deviation of the lagged normal distribution function, σ, influenced the width of the function at the level of 68% of the value of the peak intensity. This parameter was representative of the transition time between injection in-flow to the washout phases of the flow of contrast from the ROIs. A smaller value of σ signifies that the transition from inflow to the onset of washout was reduced, indicative of more efficient convective transport of the contrast.

The contrast agent had fluidic properties that differ from blood. Specifically, the contrast offered higher viscosity and specific gravity than whole blood. Moreover, the injection produced time-dependent changes in the observed flow. However, these deviations were not sufficient to preclude the analysis of contrast transport through the ROI and its extrapolation to blood flow characterization therein [17]. With consistent control over imaging and injection parameters, relative differences were quantified by the modeling process.

E. Statistical Analysis

The results are expressed as mean ± standard error of the mean. The Mann–Whitney nonparametric analysis of the variance between two means was employed to compare the differences of the model parameters between the control and treated cohorts. A repeated measures analysis of the variance (two-factor repeated ANOVA) with a Tukey–Kramer multiple comparison posttest was employed to make comparisons of a given parameter within each group at different time points (baseline, PS, and one-week follow-up). A value of $p < 0.05$ was interpreted as statistical significance.

III. Results

Large conducting arteries including the internal and external iliac, femoral, deep femoral, inferior epigastric, lateral circumflex, popliteal, and saphenous arteries are clearly visible in the baseline angiogram [Fig. 1(A)]. As the contrast is slowly transported into the smaller arterioles, more branch generations become visible in the late phase of the angiographic sequence [Fig. 1(B)].

After the ligation and excision of a segment of the femoral artery, no branches of the external iliac artery are available for blood transport [Fig. 1(C)]. The only artery that remains for perfusion of the limb is the internal iliac artery. At a later time point in the angiographic sequence, the previous appearance of angiographic blush appears to have been nearly eliminated [Fig. 1(D)]. Ischemia of the hindlimb is acutely severe. Normally occurring anastomoses between the inferior gluteal and deep femoral arteries perhaps maintain minimal perfusion of the hip adductor muscles and the flexor muscle groups [18], and hence explain the survival of the limb.

A comparison of the neovascular formation between the treated and control groups is shown in Fig. 4 after one week from the surgery and treatment. In the control group, smaller branches of the superior and inferior gluteal arteries become angiographically evident [Fig. 4(A)]. In the treated animal, one week following surgery numerous vessels have grown throughout the thigh, forming anastomoses with the arteries that supply the leg [Fig. 4(B)]. A myriad of vessels have sprouted from the iliolumbar, inferior, and superior gluteal arteries to perfuse the muscles of the thigh. The blush has intensified, indicating progress in development of the microvasculature.

Examples of time intensity plots with the superimposed model fitted to the data acquired with the LAM are presented in Fig. 5. The peak intensity is lowered after the surgery [Fig. 5(B)]. It also appears that the time to transition from inflow to washout of the contrast is delayed within the large arteries, with a longer time constant for the decay of the intensity.

The intensity curves for the angiographic blush have a lower signal-to-noise ratio than those previously examined for the large artery mask. The number of capillaries is orders of magnitude larger than the number of large conducting arteries, and thus the contrast density is dramatically reduced. This fact is demonstrated by the lower amplitude of the time intensity curve, and the decreased signal-to-noise ratio. The baseline case [Fig. 6(A)] shows a clear pattern of contrast entering and beginning to exit the capillary bed. Because the process of contrast transport within the capillaries is slow, the average inverted grayscale values cannot return to the background level within the observation period. After the surgical induction of ischemia, the blush is dramatically decreased, with a mean behavior that begins to disappear into the noise [Fig. 6(B)].

The blush peak intensity value is higher in the treated [Fig. 6(C)] animals versus the control [Fig. 6(D)] group. It is also apparent in the treated group that the lagged normal component of the model plays a more significant role than that of the control group, indicating that the process of convection in fluid transport is present amongst the treated animals. In the control group, there is little obvious convection with the intensity rapidly ramping and then approaching a constant intensity, which does not significantly decrease within the observation period.

Fig. 7 shows the statistical comparison of the model parameters. The results show that following the onset of ischemia, the transition time (σ) significantly increases in both the control and treated groups ($p < 0.01$) [Fig. 7(A)], implying that the blood transport through the large arteries has diminished. After one week, there is a significant decrease of the

transition time in the treated animals as compared to the postsurgical time point ($p < 0.01$) and no statistically different change in the control group.

After ischemia is induced, the peak intensity of the LAM is significantly lessened for both cohorts ($p < 0.01$) [Fig. 7(B)] as the total amount of contrast flowing into the limb is diminished. At one week after surgery the peak intensity, the sum of ρ_1 and ρ_2, from the time intensity curves of the treated animals is significantly larger than those acquired immediately after surgery ($p < 0.01$). The control group also had a statistically significant change of the peak intensity within the same time period ($p < 0.05$). While difference in peak intensity between the treated and control group one week following surgery can be observed, it did not reach statistical significance ($p < 0.01$).

The peak intensity values of the blush, the sum of ρ_1 and ρ_2, decreased significantly for both the control and treated groups after surgery ($p < 0.05$) [Fig. 7(C)]. Moreover, the peak intensity derived from the treated animals was significantly larger one week after surgery ($p < 0.01$). The control group did not have a significant increase in blush intensity one week after onset of ischemia.

Counting the pixels of unity that form the large artery mask is a method of quantifying the area that the large arteries occupy within the ROI. It is analogous to the determination of the angiographic score, with the advantage that it eliminates intraobserver variability and considers more than simply the number of vessels. In this study, the pixel count decreased significantly after the surgical ligation of the external iliac artery and partial resection of the femoral artery in both groups of animals ($p < 0.01$) [Fig. 7(D)]. One week following surgery, the animals treated with VEGF have a significantly larger number of pixels forming the large artery mask than they had immediately after surgery ($p < 0.001$). However, the control group offered no significant changes in the pixel count.

IV. Discussion

The standard method for angiographically quantifying angiogenesis in both the clinical and research settings is the determination of an angiographic score. The image of an angiographic sequence that best depicts the vasculature is selected and a grid overlay is superposed. The angiographic score is defined as the number of vessels that are found within the squares divided by the total number of squares within a selected region and multiplied by 100 [19], [20]. This is a method frequently applied in preclinical therapeutic angiogenesis studies. To improve image quality resulting from sequences taken in the rabbit hindlimb ischemia model, post mortem angiography has been described [21], [22]. After sacrificing the rabbits, a buffer containing adenosine is perfused into the lower limbs from a catheter placed in the distal aorta to achieve maximal vasodilation. Contrast medium containing bismuth and gelatin is slowly infused and allowed to gel by placing the limbs on ice. The resulting angiograms provide high image quality. There is a variation of vessel counting that uses a vertical line intersecting the center of the femur, and the number of vessels crossing this line is determined [13], [23]. Standard angiographic equipment detects vessels that are larger than 250 μm [20]. Microangiographic assessment has been described when employing the rat or murine hindlimb ischemia models, and with this equipment has the capacity to detect vessels as small as 30 μm [24]–[27].

Detailed morphologic analysis of neovasculature visualized angiographically has been performed in the rabbit hindlimb ischemia model [28] and chorioallantoic membranes of chick embryos [29], [30]. A procedure to filter and thereby improve the signal-to-noise ratio was performed on digitally subtracted angiographic images of chick chorioallantoic membranes [29]. The thesis of this work was that grayscale intensity is proportional to the

vessel size, and therefore image histograms permit classification of the vessel diameters present in the image. Skeletonized binary images gave vessel lengths by pixel counting. Thus, for a singular image geometric parameters of the neovasculature were assessed. A more complex analysis utilizing fractal geometric methods has been carried out for quantitative assessment of angiogenesis in the rabbit hindlimb ischemia model and chorioallantoic membranes of chick embryos [28], [30]. From this analysis indices of vascular complexity and density were determined to assess the level of angiogenesis. These morphometric studies performed on a single angiogram allow only for the analysis of geometric information, neglecting a temporal assessment of contrast motion through the neovasculature.

The process of arteriogenesis involves the development of large arteries with the primary function of convecting blood to distal capillary beds. Angiogenesis is the sprouting of new microvessels in order to supply ischemic tissues directly. The methodology of analyzing angiographic data presented herein specifically addresses these two mechanisms of neovascular growth. By modeling the temporal changes in contrast transport using the large artery mask, it may be conceived that this is a means to quantify the process of arteriogenesis; whereas, applying a similar modeling process to the grayscale data acquired with the blush mask examines the microvessel development and hence pertains largely to angiogenesis.

Modeling dispersion of an indicator in the human circulation with a lagged normal model was first reported by Bassingtwaighte *et al.* [31]. This method of modeling was later applied by Bassingtwaighte to model indicator-dilution curves in the arteries of the human leg [32]. The technique varies in this study in that the time intensity curves represent the output, which is modeled directly. Moreover, a second term is included in the model to account for the late phase of the time intensity curve which is the accumulation of contrast within the ROI that has not had sufficient time to clear within the observation period. An average error, defined as the root of the summed differences between the square of the model predictions and the data values, divided by the root mean square of the data, was 6.7% for the model fit to the data extracted from the large artery mask. Thus, results from past reports and the current analysis prove that this model has been appropriately selected and applied.

The model parameter σ is coupled in both terms of the model. This parameter is the standard deviation of the lagged normal component of the model, and it represents the time elapsed as the flow enters the ROI and then begins to washout. This model parameter is also included in the modified error function, which is the second term of the model. In this term of the model,σ influences the time of transition between the baseline intensity and the peak intensity. Using the large artery mask, a comparison of the relative magnification coefficients for the lagged normal and modified error function components of the model, ρ_1 and ρ_2, respectively, it is clear that the first term is dominant. This is a reasonable observation in that the large arteries convect blood for distribution into distal vascular beds. Hence, the modeling of contrast transport within these arteries is predominantly related to convection, or bulk fluid motion, which is described by the lagged normal component of the model. From this interpretation, σ is indicative of the capacity of these arteries to perform the function of bulk blood transport. A smaller value of the transition time implies that the blood is rapidly transported within the given ROI.

The transition time may be posited to be inversely proportional to the regional blood flow, since more efficient transport of blood to the distal tissues occurs. The results shown in Fig. 7(A) correlate well to the large study performed by Gowdak *et al.* [20]. Rabbits that received cationic lipid-mediated VEGF gene transfer (1000 μg) had a significantly larger regional blood flow to the adductor and gastrocnemius muscles at one and two week endpoints than

did the control group, as measured with radioactive microspheres. These results in comparison to those presented herein tend to support the hypothesis that the transition time might be inversely proportional to regional blood flow.

The sum of the amplification coefficients, ρ_1 and ρ_2, is related to the total amount of contrast, and hence the total amount of blood, that enters the ROI. After ischemia is induced, the peak intensity is significantly lessened. Taken together, the significant increase in the amplification factor and decrease of the transition time indicate that the treated animals have a larger amount of blood flowing more rapidly through the affected limb than the control group.

The pixel count [Fig. 7(D)] is shown in order to compare the large artery mask to angiographic scores of previous studies. In these experiments, the treated group had a significant increase in the number of pixels that form the LAM than the control group after one week of ischemia. This result is in direct agreement with multiple reports in which treatments using either recombinant human VEGF protein or naked plasmid DNA expressing VEGF demonstrated improvements in angiographic score as compared to controls [13], [14], [20], [28], [33]–[35].

The modeling of time intensity data representing angiographic blush was attempted with a sum of the lagged normal model and the modified error function. The relative contribution of each component of this model was similar, and hence it may not be optimal to couple these terms with the same model parameters. However, using separate model parameters for each component of the model resulted in insignificant differences in the model parameters from the baseline angiographic sequences to those acquired after the onset of ischemia. The independency of the model parameters on changes in the data implies that the model is not parsimonious, and the model should be simplified. Simplifying the model to include only the modified error function misrepresented certain time intensity curves, particularly those acquired from the treated animals.

No clear trends or significant differences of the model parameters between the treated and control groups were observed in the blush, excluding the peak intensity value. The peak intensity values, the sum of ρ_1 and ρ_2, increased significantly from ischemia onset to one week after surgery in the treated group. Moreover, the peak intensity derived from the treated animals was significantly larger than that of the control group one week after surgery ($p < 0.01$). The peak intensity obtained using the blush mask is related to the microvascular density within the ROI. This assertion is based on the premise that increased microvasculature is demonstrated angiographically by the augmented presence of blush. Therefore, the increased peak intensity observed after one week is hypothesized to represent a higher density of the microvasculature. This finding is supported by the results of many studies wherein histological measurements revealed that after one week VEGF-treated animals had a significantly higher vascular density than did the controls [14], [20], [33], [34].

Therapeutic angiogenesis has proven in both preclinical and clinical research a benefit in the treatment of ischemic disease. Gene therapy employed to express angiogenic growth factors may eventually be one of the best means to achieve reperfusion of ischemic tissues. For the continued development of this technology, an accurate and objective modality to quantify the levels of angiogenesis that may be used clinically is required. This modality should be able to assess hemodynamic changes as well as the numbers and geometry of the newly formed vessels. Previously, angiographic analysis of therapeutic angiogenesis has been confined to the extraction of geometric information and the enumeration of opacified vessels from a singular image. The methodology presented in this paper is one proposed solution to

quantify angiogenesis angiographically in both the research lab and the clinical angiosuite, and to provide a means of both geometric and hemodynamic analyses.

Acknowledgments

The authors extend their gratitude to the expert support provided to this project by B. Jay Wasserlauf, Dr. Liliana Cesar, and Dr. Howard M. Prentice.

This work was supported by the NIH RO1 HL072924-01 (KAW), Siemens America Medical Solutions (AKW), and an endowed chair from the Walter G. Ross Foundation (to KAW).

References

1. Isner JM, Asahara T. Angiogenesis and vasculogenesis as therapeutic strategies for postnatal neovascularization. J. Clin. Invest. 1999; vol. 103:1231–1236. [PubMed: 10225965]
2. Schainfeld RM, Isner JM. Critical limb ischemia: Nothing to give at the office. Ann. Intern. Med. 1999; vol. 130:442–444. [PubMed: 10068420]
3. Rivard A, Fabre JE, Silver M, Chen D, Murohara T, Kearney M, Magner M, Asahara T, Isner JM. Age-dependent impairment of angiogenesis. Circulation. 1999; vol. 99:111–120. [PubMed: 9884387]
4. Isner JM. Manipulating angiogenesis against vascular disease. Hosp. Pract. 1999; vol. 34:69–74.
5. Lewis BS, Flugelman MY, Weisz A, Keren-Tal I, Schaper W. Angiogenesis by gene therapy: A new horizon for myocardial revascularization. Cardiovasc. Res. 1997; vol. 35:490–497. [PubMed: 9415293]
6. Melillo G, Scoccianti M, Kovesdi I, Safi J Jr, Riccioni T, Capogrossi MC. Gene therapy for collateral vessel development. Cardiovasc. Res. 1997; vol. 35:480–489. [PubMed: 9415292]
7. Webster KA. Therapeutic angiogenesis: A case for targeted, regulated gene delivery. Crit. Rev. Eukaryot Gene Expr. 2000; vol. 10:113–125. [PubMed: 11186327]
8. Baumgartner I, Pieczek A, Manor O, Blair R, Kearney M, Walsh K, Isner JM. Constitutive expression of phVEGF165 after intramuscular gene transfer promotes collateral vessel development in patients with critical limb ischemia. Circulation. 1998; vol. 97:1114–1123. [PubMed: 9537336]
9. Fortuin FD, Vale P, Losordo DW, Symes J, DeLaria GA, Tyner JJ, Schaer GL, March R, Snell RJ, Henry TD, Van Camp J, Lopez JJ, Richenbacher W, Isner JM, Schatz RA. One-year follow-up of direct myocardial gene transfer of vascular endothelial growth factor-2 using naked plasmid deoxyribonucleic acid by way of thoracotomy in no-option patients. Amer. J. Cardiol. 2003; vol. 92:436–439. [PubMed: 12914874]
10. Isner JM, Pieczek A, Schainfeld R, Blair R, Haley L, Asahara T, Rosenfield K, Razvi S, Walsh K, Symes JF. Clinical evidence of angiogenesis after arterial gene transfer of phVEGF165 in patient with ischaemic limb. The Lancet. 1996; vol. 348:370–374.
11. Losordo DW, Vale PR, Symes JF, Dunnington CH, Esakof DD, Maysky M, Ashare AB, Lathi K, Isner JM. Gene therapy for myocardial angiogenesis: Initial clinical results with direct myocardial injection of phVEGF165 as sole therapy for myocardial ischemia. Circulation. 1998; vol. 98:2800–2804. [PubMed: 9860779]
12. Yao Q, Wang S, Gambotto A, Glorioso JC, Evans CH, Robbins PD, Ghivizzani SC, Oligino TJ. Intra-articular adenoviral-mediated gene transfer of trail induces apoptosis of arthritic rabbit synovium. Gene Therapy. 2003; vol. 10:1055–1060. [PubMed: 12776164]
13. Becit N, Ceviz M, Kocak H, Yekeler I, Unlu Y, Celenk C, Akin Y. The effect of vascular endothelial growth factor on angiogenesis. An experimental study. Eur J. Endovasc. Surg. 2001; vol. 22:310–316.
14. Bauters C, Asahara T, Zheng LP, Takeshita S, Bunting S, Ferrara N, Symes JF, Isner JM. Site-specific therapeutic angiogenesis after systemmic administration of vascular endothelial growth factor. J. Vasc. Surg. 1995; vol. 21:314–325. [PubMed: 7531786]
15. Li Z, Lieber BB. Estimation of organ transport function: Model-free deconvolution by recursive quadratic programming optimization. J. Biomech. Eng. 1992; vol. 114:482–489. [PubMed: 1487900]

16. Sadasivan C, Lieber BB, Gounis MJ, Lopes DK, Hopkins LN. Quantification of stent efficacy in modulating angiographic dye washout from cerebral aneurysms. AJNR Amer. J. Neuroradiol. 2002; vol. 23:1214–1222. [PubMed: 12169482]

17. Eigler NL, Pfaff M, Zeihar A, Whiting JS, Forrester JS. Digital angiographic impulse response analysis of regional myocardial perfusion: Linearity, reproducibility, accuracy, and comparison with conventional indicator dilution curve parameters in phantom and canine models. Circ. Res. 1989; vol. 64:853–866. [PubMed: 2650918]

18. McNally MA, Small JO, Mollan RAB, Wilson DJ. Arteriographic study of the rabbit lower limb. Anatom. Rec. 1992; vol. 233:643–650.

19. Gowdak LHW, Poliakova L, Wang X, Kovesdi I, Fishbein KW, Zacheo A, Palumbo R, Straino S, Emanueli C, Marrocco-Trischitta M, Lakatta EG, Anversa P, Spencer RG, Talan M, Capogrossi MC. Adenovirus-mediated VEGF121 gene transfer stimulates angiogenesis in normoperfused skeletal muscle and preserves tissue perfusion after induction of ischemia. Circulation. 2000; vol. 102:565–571. [PubMed: 10920070]

20. Gowdak LHW, Poliakova L, Li Z, Grove R, Lakatta EG, Talan M. Induction of angiogenesis by cationic lipid-mediated VEGF165 transfer in the rabbit ischemic hindlimb model. J. Vasc. Surg. 2000; vol. 32:343–352. [PubMed: 10917995]

21. Deindl E, Buschmann I, Hoefer I, Podzuweit T, Boengler K, Vogel S, van Royen N, Fernandez B, Schaper W. Role of ischemia and of hypoxia-inducible genes in arteriogenesis after femoral artery occlusion in the rabbit. Circ. Res. 2001; vol. 89:779–786. [PubMed: 11679407]

22. Hoefer I, van Royen N, Buschmann I, Piek JJ, Schaper W. Time course of arteriogenesis following femoral artery occlusion in the rabbit. Cardiovasc. Res. 2001; vol. 49:609–617. [PubMed: 11166274]

23. Hong JH, Bahk YW, Suh JS, Kwak BK, Shim HJ, Kim JS, Kim HS, Moon YH, Kim SJ, Chung JW, Park JH. An experimental model of ischemia in rabbit hindlimb. J. Korean Med. Sci. 2001; vol. 16:630–635. [PubMed: 11641535]

24. Silvestre JS, Mallat Z, Tamarat R, Duriez M, Tedgui A, Levy BI. Regulation of matrix metalloproteinase activity in ischemic tissue by interleukin-10. Circ. Res. 2001; vol. 89:259–264. [PubMed: 11485976]

25. Takeshita S, Isshiki T, Mori H, Tanaka E, Tanaka A, Umetani K, Eto K, Miyazawa Y, Ochiai M, Sato T. Microangiographic assessment of collateral vessel formation following direct transfer of vascular endothelial growth factor in rats. Cardiovasc. Res. 1997; vol. 35:547–552. [PubMed: 9415300]

26. Takeshita S, Isshiki T, Mori H, Tanaka E, Eto K, Miyazawa Y, Tanaka A, Shinozaki Y, Hyodo K, Ando M, Kubota M, Tanioka K, Umetani K, Ochiai M, Sato T, Miyashita H. Use of synchrotron radiation microangiography to assess development of small collateral arteries in a rat model of hindlimb ischemia. Circulation. 1997; vol. 95:805–808. [PubMed: 9054734]

27. Takeshita S, Isshiki T, Ochiai M, Eto K, Mori H, Tanaka E, Umetani K, Sato T. Endothelium-dependent relaxation of collateral microvessels after intramuscular gene transfer of vascular endothelial growth factor in a rat model of hindlimb ischemia. Circulation. 1998; vol. 98:1261–1263. [PubMed: 9751672]

28. Hopkins SP, Bulgrin JP, Sims RL, Bowman B, Donovan DL, Schmidt SP. Controlled delivery of vascular endothelial growth factor promotes neovascularization and maintains limb function in a rabbit model of ischemia. J. Vasc. Surg. 1998; vol. 27:886–895. [PubMed: 9620141]

29. Karnabatidis D, Dimopoulos JCA, Siablis D, Papazafiropoulos D, Kalogeropoulou CP, Nikiforidis G. Quantification of the ionising radiation effect over angiogenesis in the chick embryo and its chorioallantoic membrane by computerised analysis of angiographic images. Acta Radiol. 2001; vol. 42:333–338. [PubMed: 11350295]

30. Kirchner LM, Schmidt SP, Gruber BS. Quantitation of angiogenesis in the chick chorioallantoic membrane using fractal analysis. Microvasc. Res. 1996; vol. 51:2–14. [PubMed: 8812748]

31. Bassingthwaighte JB, Ackerman FH, Wood EH. Applications of the lagged normal density curve as a model for arterial dilution curves. Circ. Res. 1966; vol. 18:398–415. [PubMed: 4952948]

32. Bassingthwaighte JB. Plasma indicator dispersion in arteries of the human leg. Circ. Res. 1966; vol. 19:332–346. [PubMed: 5330717]

33. Bauters C, Asahara T, Zheng LP, Takeshita S, Bunting S, Ferrara N, Symes JF, Isner JM. Physiological assessment of augmented vascularity induced by VEGF in ischemic rabbit hindlimb. Amer. J. Physiol. 1994; vol. 267:H1263–H1271. [PubMed: 7943370]

34. Takeshita S, Weir L, Chen D, Zheng LP, Riessen R, Bauters C, Symes JF, Ferrara N, Isner JM. Therapeutic angiogenesis following arterial gene transfer of vascular endothelial growth factor in a rabbit model of hindlimb ischemia. Biochem. Biophys. Res. Commun. 1996; vol. 227:628–635. [PubMed: 8878563]

35. Asahara T, Bauters C, Zheng LP, Takeshita S, Bunting S, Ferrara N, Symes JF, Isner JM. Synergistic effect of vascular endothelial growth factor and basic fibroblast growth factor on angiogenesis in vivo. Circulation. 1995; vol. 92:365–371.

Biographies

Matthew J. Gounis received the M.S. degree in 2001 in mechanical engineering from the State University of New York at Buffalo, Buffalo, NY, and the Ph.D. degree in 2004 in biomedical engineering from the University of Miami, Coral Gables, FL.

He has previously been employed as a Principal Engineer at Cordis Neurovascular (a Johnson and Johnson company, Miami Lakes, FL). He is presently an Assistant Professor of radiology and Director of the New England Center for Stroke Research at the University of Massachusetts, Worcester. His research interests include medical imaging and image-guided therapy for cerebrovascular disease.

Dr. Gounis is a long-time member of the Bioengineering Division of the American Society of Mechanical Engineers. His work has been recognized by awards from the American Society of Mechanical Engineers, American Society of Neuroradiology, American Association of Neurological Surgeons, Johnson and Johnson, and Sigma Xi.

Baruch B. Lieber received the M.S. degree in 1982 and the Ph.D. degree in 1985, both in aerospace engineering from the Georgia Institute of Technology, Atlanta.

He has previously been employed as Professor at the State University of New York at Buffalo in the Department of Mechanical Aerospace Engineering and served as Director for the Center for Bioengineering. He is presently a Professor of biomedical engineering and radiology and Director of the Endovascular Research Center at the University of Miami, Coral Gables, FL. His research interests include experimental fluid mechanics of cerebrovascular disease and minimally invasive devices to cure cerebral aneurysms.

Dr. Lieber is a long-time member of the Bioengineering Division of the American Society of Mechanical Engineers (Fellow) and Biomedical Engineering Society. His work has been recognized by awards from the Radiological Society of North America, American Society of

Mechanical Engineers, American Society of Neuroradiology, and American Association of Neurological Surgeons.

Keith A. Webster received the Ph.D. degree in biochemistry in 1980 from the University of York, York, U.K.

He has previously been employed as Program Director, Molecular Cardiology Laboratory, SRI International. He is presently a Professor in the Department of Molecular and Cellular Pharmacology, Director of the Vascular Biology Institute, and the Walter G Ross Chair of Vascular Biology at the University of Miami, Miami, FL. His research interests include molecular mechanisms of hypoxia/ischemia-regulated gene expression, molecular pathology of vascular disease, control of cell death in ischemic heart disease/protective strategies, and gene therapy with “Intelligent Gene” delivery techniques.

Dr. Webster is a long-time member of the American Heart Association Basic Sciences Council Member, Consultant NIH National Heart Lung and Blood Institute, Fellow of the American Heart Association, Miami-Dade Community Board, and Scientific Advisory Board at Florida Atlantic University Center of Excellence.

Ajay K. Wakhloo received the medical doctorate degree in 1984 from the University of Mainz, Mainz, Germany, and the Ph.D. degree in the area of metabolic disorders in 1986. He received his habitation in 1996 at the University of Tuebingen, Tuebingen, Germany, following the publication and presentation of his novel study of the effect of stent-induced flow remodeling to treat intracranial aneurysms.

He has previously been employed as a Professor at the University of Miami in the Departments of Radiology, Biomedical Engineerin, g and Neurological Surgery. He is presently a Professor of radiology, neurology, and neurosurgery and Director of the Division of Neuroimaging and Intervention at the University of Massachusetts, Worcester. His research interests include the endovascular treatment of cerebral aneurysms, arteriovenous malformations, spinal vascular malformations, and acute stroke.

Dr. Wakhloo is a long-time member of the American Medical Association, American Society of Neuroradiology, American Society of Interventional and Therapeutic Neuroradiology, and International Academy of Clinical and Applied Thrombosis/ Hemostasis (Fellow). Dr.Wakhloo has won numerous awards for his research work and clinical practice, including most recently the Best Doctors of America.

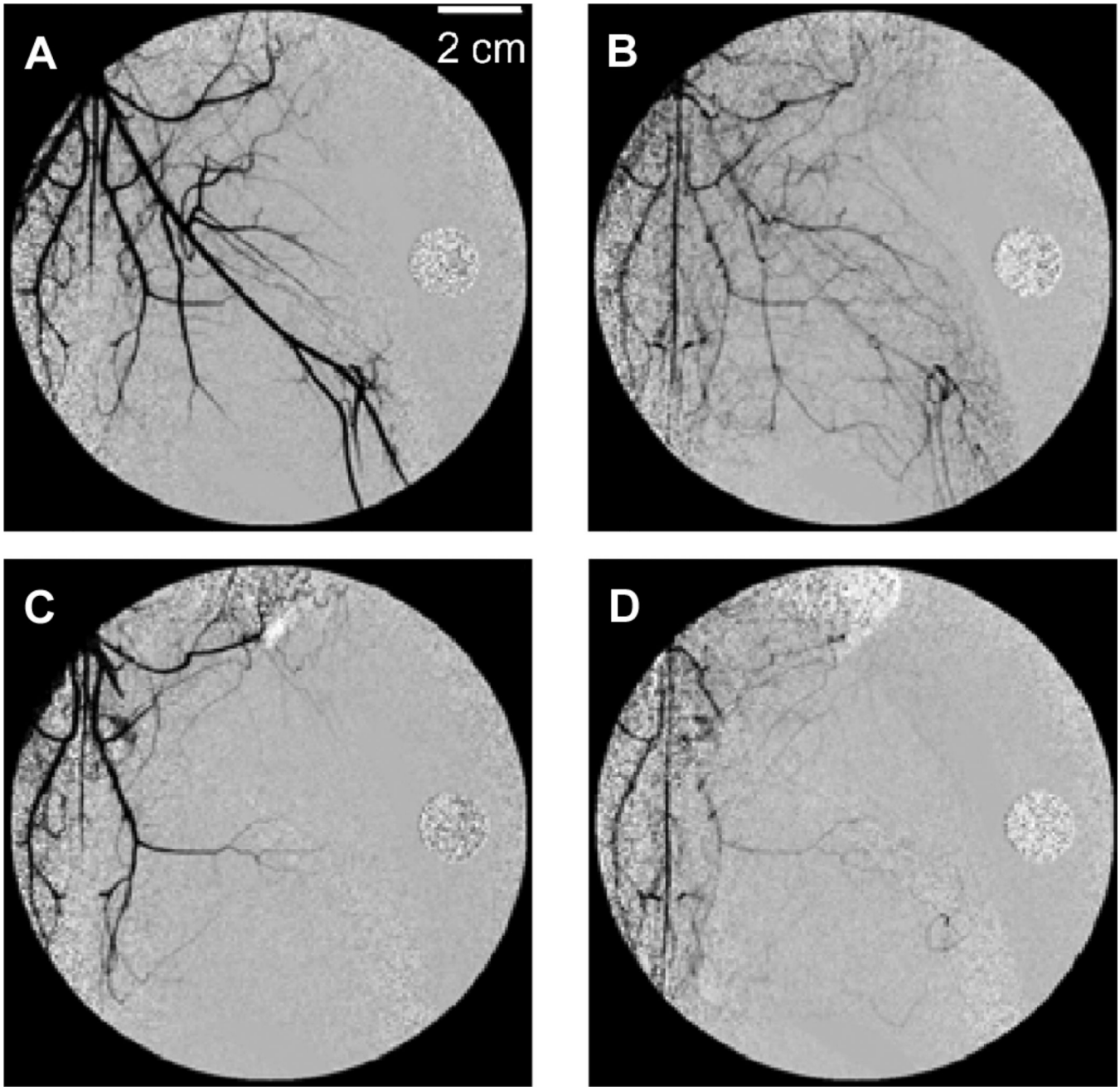

Fig. 1.
Baseline angiogram of the native vasculature of the rabbit's left hindlimb at (A) peak opacification of the contrast and (B) during the late phase of concentration decay of the contrast. After ligation of the external iliac artery and the resection of a femoral artery segment, severe ischemia to the limb is observed under (C) angiography at peak and (D) late phase contrast concentrations.

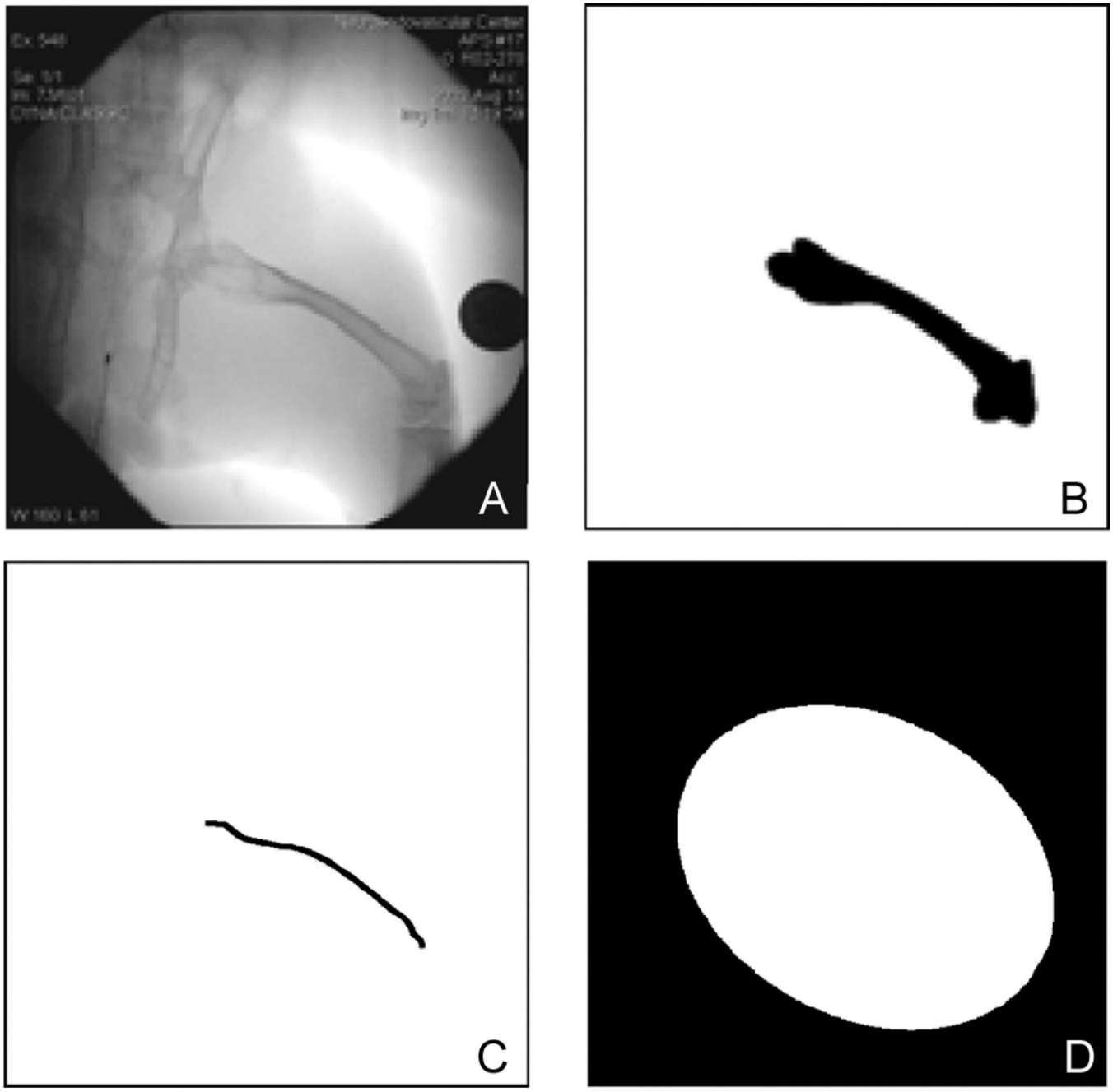

Fig. 2.

Native image of an angiographic sequence prior to contrast injections which delineates the femur (A). The femur is then isolated, thresholded and converted into a binary image (B). A skeletonizing operation is performed to reduce the femur to a single line (C). An elliptical region of interest is created based on the line that connects the endpoints of the skeletonized femur (D).

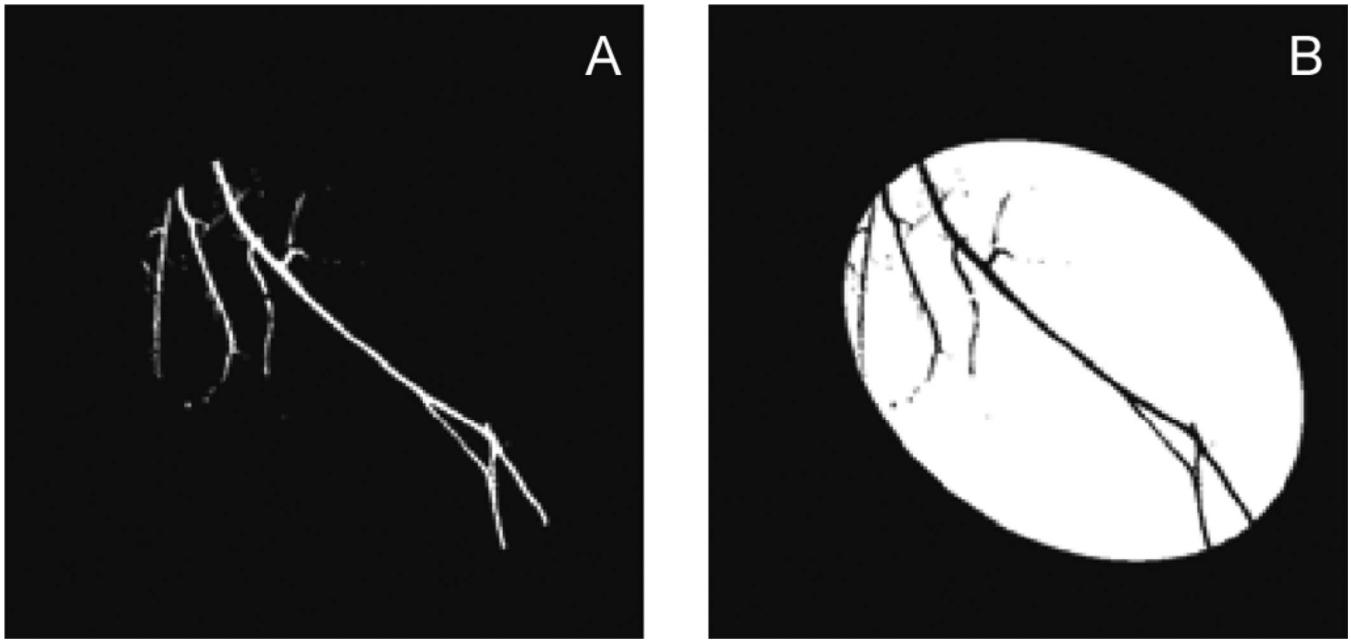

Fig. 3.
(A) Large artery mask preserves intensity changes occurring within the white region, having a pixel value of 1. The inverted mask, (B) the blush mask, captures image information outside of the large arteries.

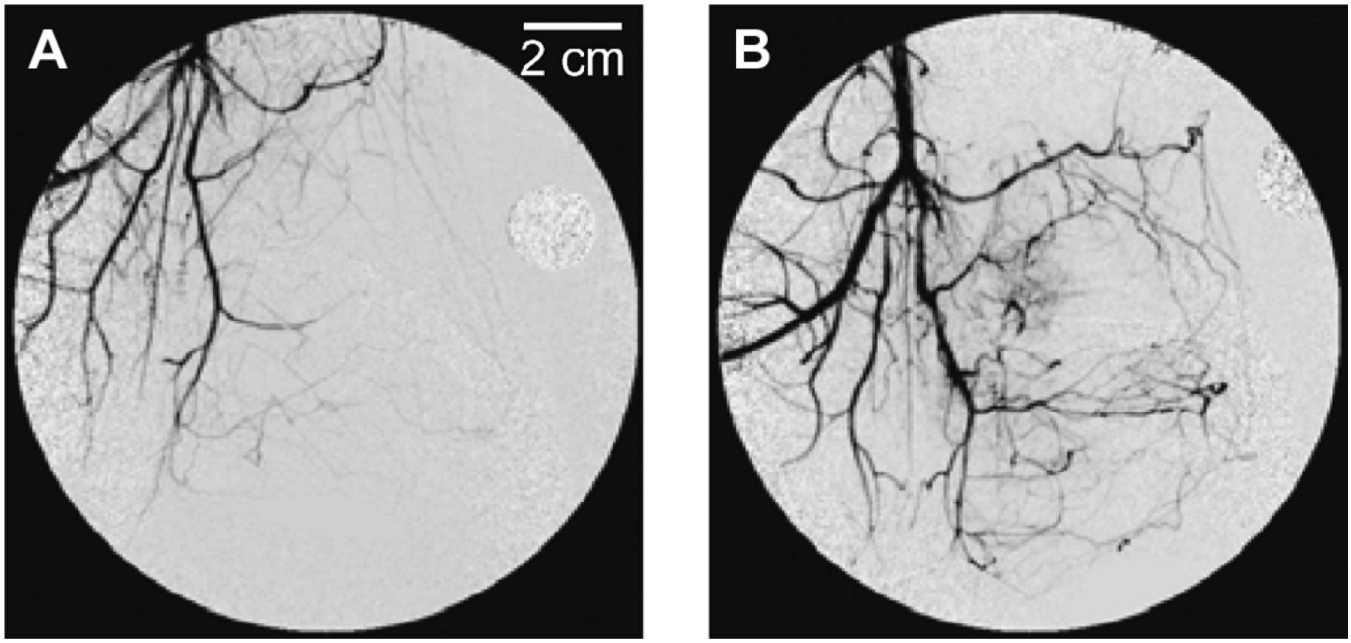

Fig. 4.
Peak opacified digitally subtracted angiograms of the ischemic hindlimb one week after surgery and injections in (A) control and (B) treated cases.

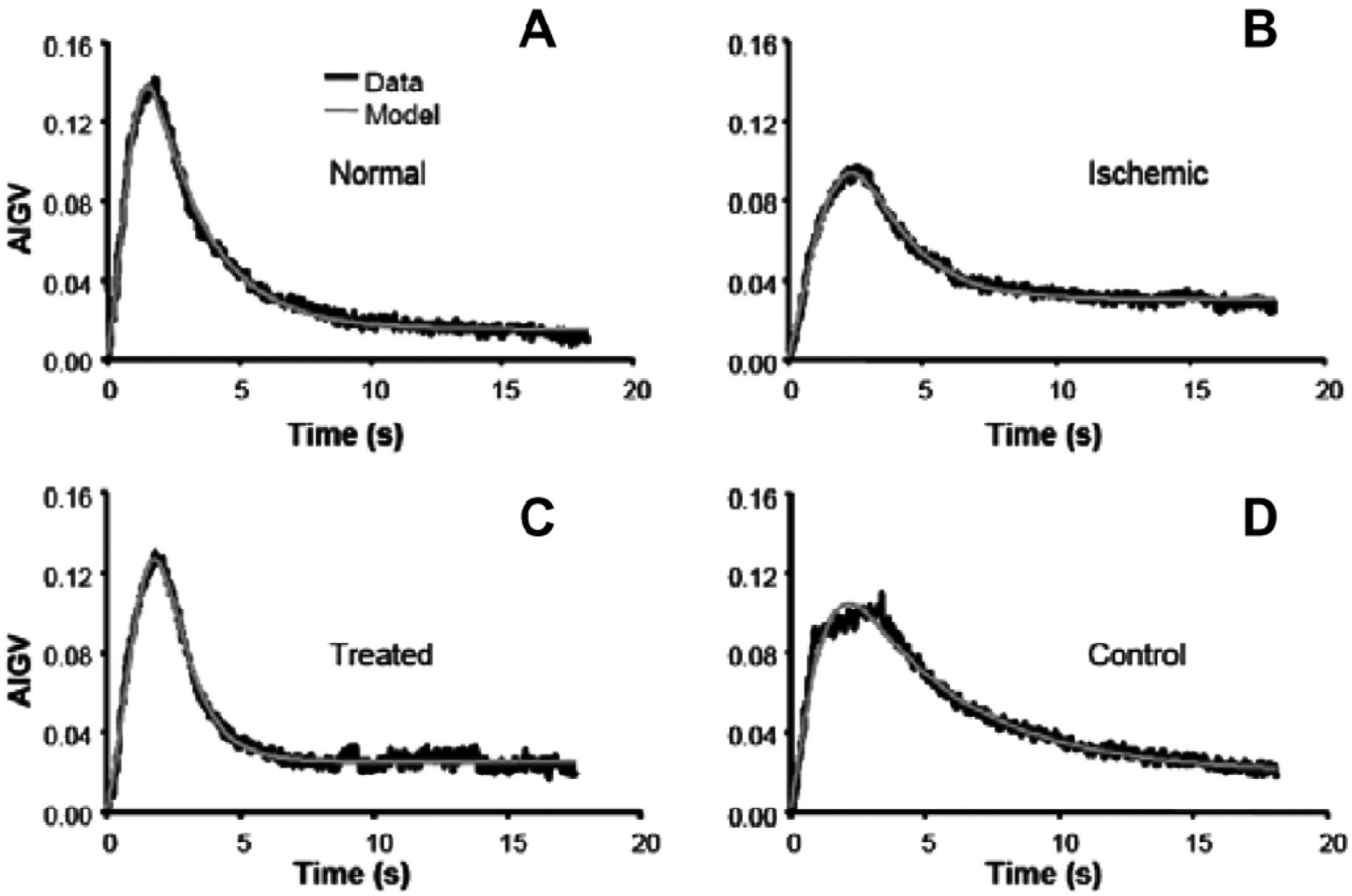

Fig. 5.

Time intensity plots obtained using the large artery mask with the optimized model fit (A) superimposed before surgery and (B) after surgical induction of ischemia. The bottom panel depicts the results for (C) treated and (D) control cases. Data are shown as average inverted grayscale values (AIGV) within the ROI.

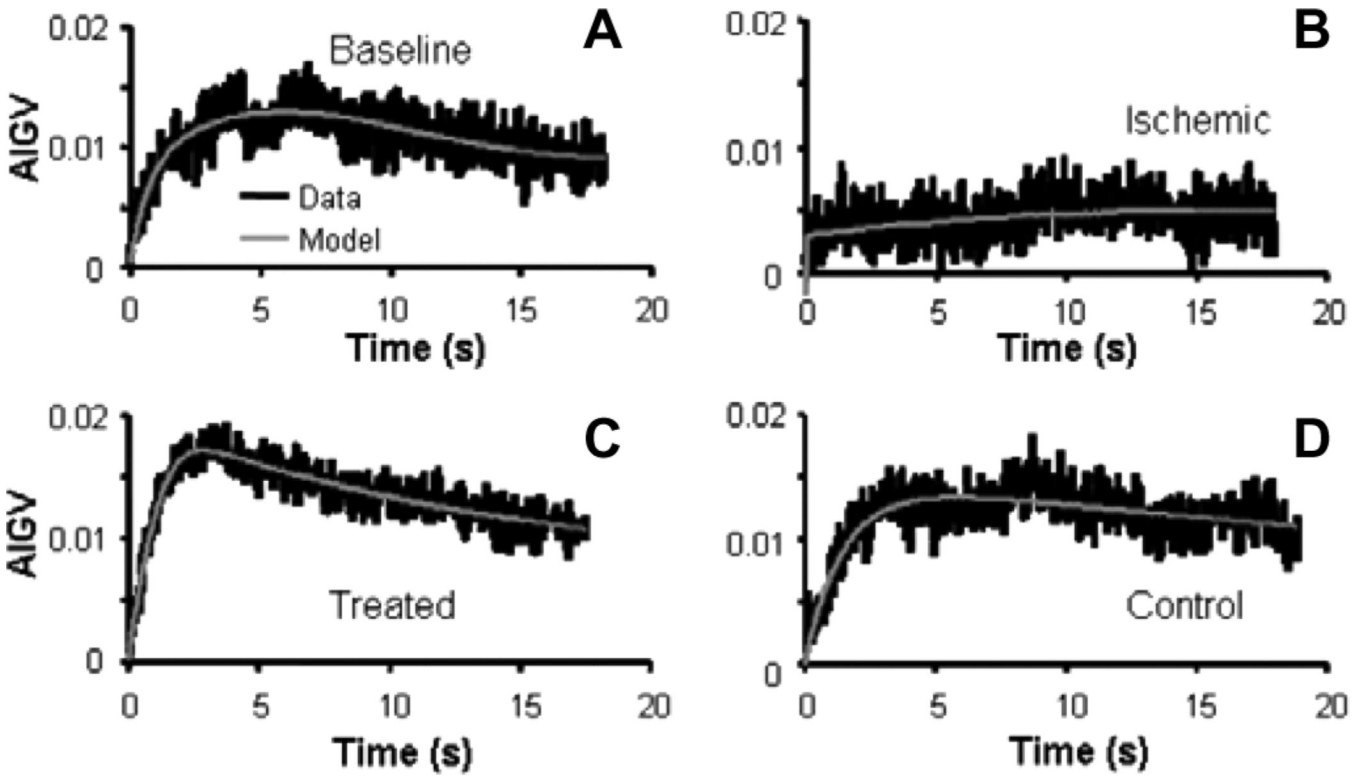

Fig. 6.

Time intensity plots obtained using the blush mask with the optimized model fit (A) superimposed before surgery and (B) after surgical induction of ischemia. The bottom panel depicts the results for (C) treated and (D) control cases. Data are shown as average inverted grayscale values (AIGV) within the ROI.

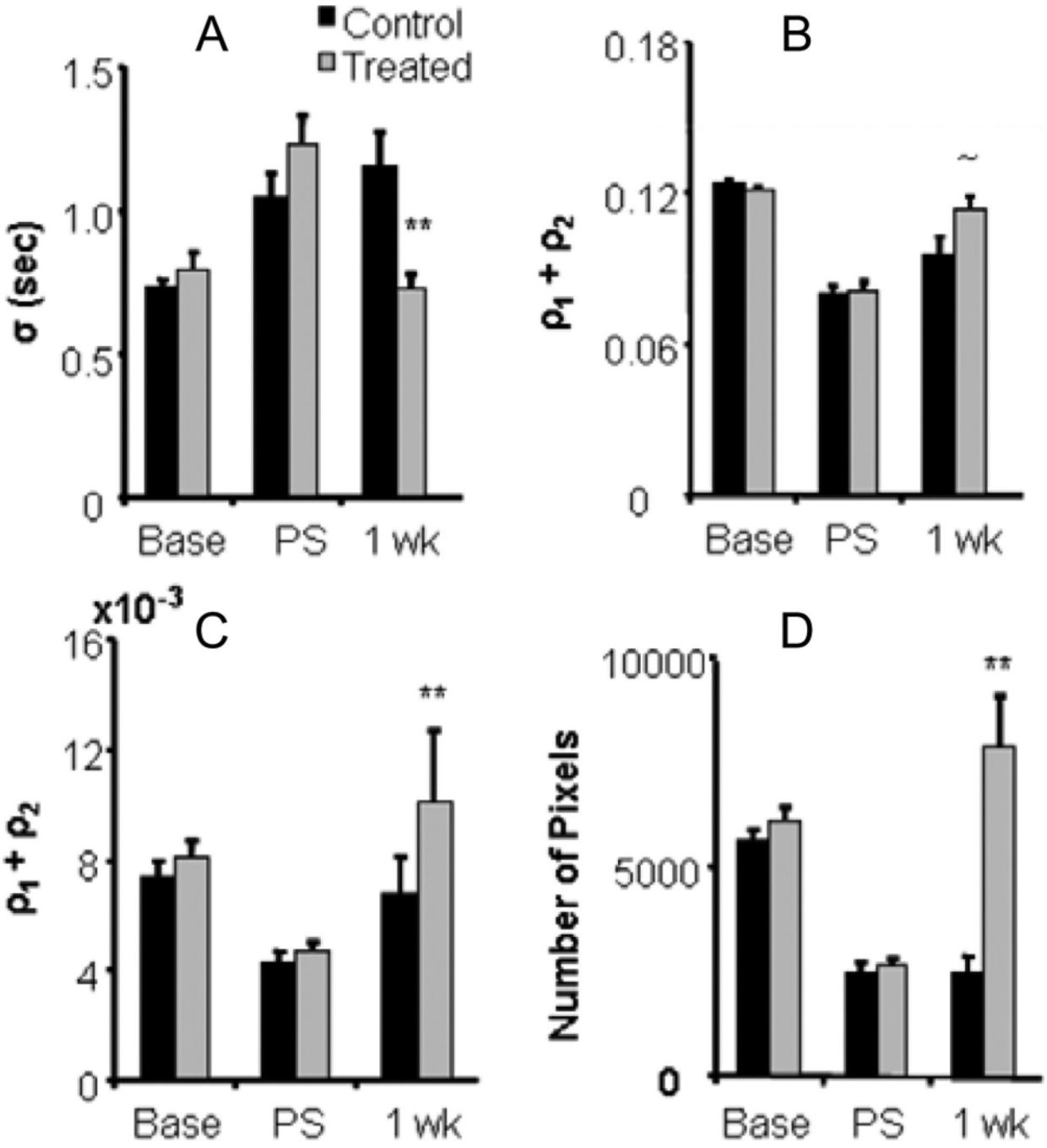

Fig. 7.

Comparison of various model parameters before surgery, after surgery, and at follow-up for the control and treated animals. Shown are the transition time of the contrast transport through (A) the large arteries and (B) the peak intensity obtained with the LAM. (C) The peak intensity of the data using the blush mask. (D) The number of pixels that form the LAM which is related to the angiographic score (~ $p < 0.1$ versus control at one week,** $p < 0.01$, versus control at one week).